International Journal of Advanced Technology and Innovative Research

ISSN 2348–2370
Vol.08,Issue.02,
February-2016,
Pages:0380-0386

www.ijatir.org

Enhancement of Dynamic Stability in Micro Grid during Isolated Mode Using Fuzzy Logic Controller

P. TEJASWI
PG Scholar, Dept of EEE, MITS College, JNTUA, Chittoor(Dt), AP, India, E-mail: tejaswi.ssits@gmail.com.

Abstract: A micro grid is a group of interconnected loads and distributed energy resources within clearly defined electrical boundaries that acts as a single controllable entity with respect to the grid.It can support the back-up power or to support the main power grid during periods of heavy demand. Micro grids are cost effective and reliable.nMajor default in wind energy generations is speed instabilities cause high deviations in the output power of a wind turbine which cause differences in frequency and voltage of the MG at islanding mode and originate stability problems. Here three methods are implemented for reducing wind speed fluctuations. In the first method, we develop a new fuzzy logic pitch angle controller for reducing the fluctuations of wind turbine output power. In Second method, we design an energy storage ultra-capacitor which can completely smoothed output power of the wind turbine. In third method we use a storage battery to reduce the problems originated by the wind power fluctuations in side the micro grid but these are having less discharging capability so we are adding solid state super capacitor, nickel cadmium batteries, DFIG and solid oxide fuel cell in micro grid.

Keywords: Fuzzy Pitch Angle Controller, Islanding, Micro Grid (MG), Storage Batteries, Ultra-Capacitor, Nickel Cadmium Batteries, DFIG And Solid Oxide Fuel Cell.

I. INTRODUCTION

Environmental vise renewable sources are reducing CO2 emission in nature. Micro grid contains two modes.

- Micro grid is connected to the main grid (distribution network).
- Islanding mode.

Islanding Mode: Micro grid is disconnected from the main grid because of some faults and disturbances at micro grid. Micro grid worked independently. Micro sources (e.g., several kinds of micro gas turbines, Fuel cells, photovoltaic (PV) panels, and wind turbines) used in MG, but these are not fit to supply energy to MG directly so interface with MG through inverter. Keeping the stability and power quality at islanding mode needs more sophisticated inverter control strategies to maintain stable frequency and voltage in the presence of randomly varying loads.

A. MG Dynamics

In [8], the authors define the possibility of a control strategy using in the operation of the MG during islanding mode. The MG having a PV panel, a storage battery, and loads was tested in a laboratory and installed in the National Technical University of Athens [12] they are measure the dynamic performance of MGs subsequent to the islanding process. Problems occurred due to wind speed fluctuations during the islanding mode are as follows.

- **Fluctuation of MG Frequency:** Generated wind power is proportional to the cube of the windSpeed.
- Voltage flicker: Reactive power absorbed by wind generators based on the value of the generated active power.
- **Instability and Poor Power Quality:** These are due to frequency fluctuation and voltage flicker.

Improving the power quality inside the MG at islanding mode by solving the above problems Occurred due to wind fluctuations. This paper consider for three issues to reduce fluctuations of wind power.

- New fuzzy logic pitch angle controller reduces the amount of wind turbine output power fluctuations.
- Energy capacitor system (ECS) smoothing the output power of wind turbine generator and reduces the frequency fluctuations.
- Using a storage battery removing the problems originated by the wind power fluctuation inside the MG.

II. ARCHITECTURE OF THE DEVELOPED MG

The MG considered in this study comprises a low-voltage network, loads, both controllable and uncontrollable micro sources, and storage devices. Controlled micro sources (e.g., micro turbines and fuel cells). The uncontrollable micro sources are the ones in which the output power depends on the weather Conditions (e.g., wind turbines and PV panels) the developed MG network consists of eight buses as shown in Fig. 1.

III. DYNAMIC MODELING OF MG COMPONENTS

All of the MG components are modeled in detail using Mat lab/Simulink environment. Detailed stand-alone models for inverters with different control strategies, single-shaft micro turbines(SSMTs), solid oxide fuel cells (SOFCs), wind generation systems, and PV panel models are

developed in our previous works [16], [17]. More descriptions about the modeling of those micro sources are available in [18]–[31]. In the following sections, we describe the inverter control strategies used in this study. In addition, we describe the wind generation system in detail.

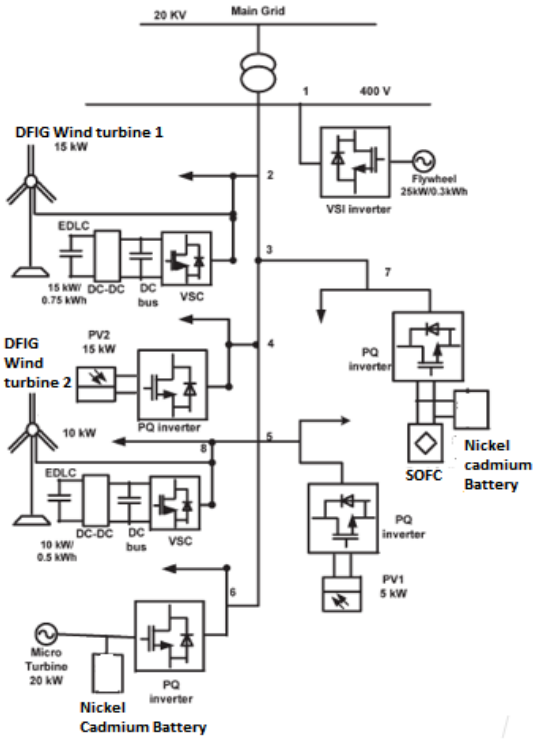

Fig.1. Architecture of the developed Micro Grid.

A. Inverter Modeling

Inverters play a major role interfacing the micro sources to the MG. In this study, two control strategies are developed to control and operate the inverters.

PQ Inverter Control: These are used to inject certain active and reactive power set points. It is used to interface SSMT, SOFC, and two PV panels. The basic structure of the PQ inverter is shown in Fig. 2. Prefin Fig. 2 represents the active power produced by the micro source which is interfaced to the MG by this inverter. Qref represents the amount of reactive power injected to or absorbed from the MG at the inverter bus. In this study, all PQ inverters operate with unity power factor to reduce their rating and cost.

VSI Control: Mg is interfaced with flywheel with help of voltage-source inverter (VSI). The output frequency and voltage of the inverters follow the droop and represents the reference bus for the MG at islanding mode VSI performed as a voltage source, with the magnitude and frequency of the output voltage controlled through droops characteristics as shown in Fig. 3. Described in the following equation

$$f = f_0 - k_p * Pf$$
$$V = V_0 - K_Q * Q \quad (1)$$

Where P and Q are the inverter active output power and reactive output power, kPand kQare the droop slopes (positive quantities), and f_0and V_0are the idle values of the frequency and voltage (nominal frequency and voltage).

B. Flywheel Modeling

To balance the system, disturbances and/or significant load changes storage devices are able to provide the amount flywheels and batteries, are modeled as constant-dc-voltage sources which, by using of power required. Storage devices, such as flywheels and batteries, are modeled as constant-dc-voltage sources which, by using power electronic interfacing, can be coupled to the MG.

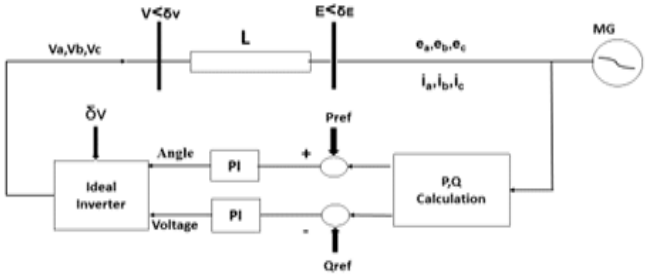

Fig. 2. Basic structure of the PQ inverter control scheme.

C. Wind Generation System Modeling

Squirrel-cage induction generators are utilized in this paper and directly connected to the MG. The stiffness of the drivetrain is infinite. The friction factor and inertia of the turbine are combined with those of the generators coupled to the turbine. The turbine output power is calculated as

$$P_m = C_p(\lambda, \beta)\, pa/2 v wind \quad (2)$$

Where
P_mMechanical output power of the turbine (in watts);
C_pPerformance coefficient of the turbine;
υwind wind speed (in meters per second);
λ ratio of the rotor blade tip speed to wind speed;
β blade pitch angle (in degrees);
A turbine swept area (in square meters).
A generic equation which is used to modelC_p(λ, β) is

$$C_p(\lambda, \beta) = C_1(C_2/\lambda_i - C_3\beta - C_4)\, e^{\frac{-C_5}{\lambda_i}} + C_6\lambda \quad (3)$$

With

$$1/\lambda_i = 1/\lambda + 0.08\beta - 0.035/\beta^3 + 1. \quad (4)$$

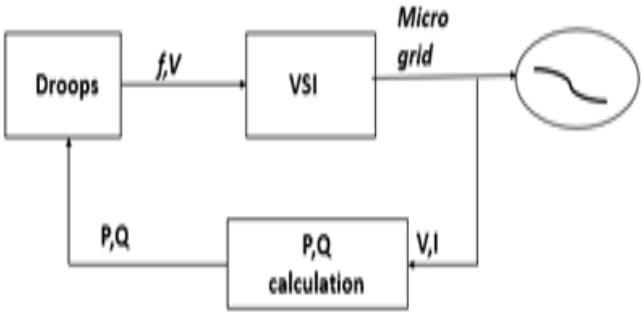

Fig. 3. VSI with droop characteristics.

The coefficients C_1 to C_6 be available. The wind turbine characteristics used in this study for different values of pitch angle (β) were described in detail in our previous work in [15]. For the induction generator, the fourth-order d_q model expressed in the arbitrary reference frame and rotating with an angular velocity ω is used. All parameters and Ratings of the two wind generation systems used in this study are available in [15].

IV. FUZZY LOGIC PITCH ANGLECONTROLLER

It can decreases amount of wind fluctuations at any value of speed by using several types of average value of the output wind power.

A. Calculation of Controller Input Power Command

For smoothing the wind generator output power, used to find the pitch controller input power command(P_{IG}^{REF}) value is find for the wind generator output power. For conventional PI pitch angle controller, that value is taken as 1 p.u. (rated power) as shown in Fig. 4. To give the effectiveness of proposed controller three types of average values are evaluated. The three types of average are described as follows.

Average Signal (AVG): Aftera specific number of periods average signal value is calculated. For example, when 20 measurementsM_1,M_2, M_{20} are taken, the successive four-period average values are calculated as follows:

$$AVG_4=(M_4+M_3+M_2+M_1)/4$$
$$AVG_8=(M_8+M_7+M_6+M_5)/4$$
$$\vdots$$
$$AVG_{20}=(M_{20}+M_{19}+M_{18}+M_{17}) \quad (5)$$

SMA: The n-period simple moving average (SMA) with a period d is calculated from

$$SMA_d=\sum_{i=1}^{n} M(\hat{d}-i)+\hat{1}/n. \quad (6)$$

If 20 measurements M1 through M20 are available, then the successive four-period SMAs are calculated as follows:

$$AVG_4=(M_4+M_3+M_2+M_1)/4$$
$$AVG_5=(M_5+M_4+M_3+M_2)/4$$
$$\vdots$$
$$AVG_{20}=(M_{20}+M_{19}+M_{18}+M_{17})/4 \quad (7)$$

EMA: The exponential moving average (EMA) is measured from the following equation:

$$EMA(C)=[(C-P)*k]+P \quad (8)$$

Where
C current value;
P previous period's EMA;
Kweighting factor.
For a period-based EMA, "k" can be calculated as

$$k=2/(1+N). \quad (9)$$

Fig. 5 shows the three mentioned average values against time for a certain pattern of wind speed. The following steps explain the calculations of the input power command P_{IG}^{REF} of the pitch controller using EMA.

Step 1: The wind turbine captured power$P_m WT$ is calculated by (2).
Step 2: the average value of the wind turbine captured power $P_m$is calculated from (8).
Step 3: the standard deviation is calculated as follows

$$\overline{P_m}\mathrm{WT}\sigma=\sqrt{\frac{\int_{t-T}^{t}(PmWT-PmWT)^2}{T}}. \quad (10)$$

Step 4: finally, the controller revised input power command PREFIG is given by

$$P_{IG}^{REF}=\overline{P_{mWT}}-P_{mWT}. \quad (11)$$

The whole process is shown in the upper part of Fig. 6.

B. Pitch Controller Design Phase

Fuzzy logic pitch controller, the turbine blade pitch angle is controlled even when the wind speed is below the rated speed. The proposed pitch controller is shown in Fig. 6. The pitch controller input power command P_{IG}^{REF} is generated from the EMA value of the wind turbine captured power as explained in the upper part of Fig. 6. Then, the difference between PIGREF and PIG (the actual generated power) is progressed through an FLC to generate the command signal β_{cmd} for the mechanical servo system. For convenience, the inputs and outputs of the FLC are scaled with coefficientsK_e, $K\Delta_e$, and K_β. The values of K_e,$K\Delta_e$, and $K_\beta$are five, six, and ten, respectively. The triangular membership functions with overlap are used for the inputs and outputs as shown in Fig. 7. The linguistics is represented by negative large (NL), negative medium (NM), negative small (NS), zero (ZO), positive small (PS), positive medium (PM), and positive large (PL). The entire rule base is given in Table I. There is a total of 49 rules to achieve the desired angle β_{cmd}. Mamdani's max–min was used for the inference mechanism. The center-of-gravity method is used for defuzzification to obtain β_{cm}.

C. ECS

The schematic diagram of the ECS is shown in Fig. 8. ECS contains three main parts;

- Pulse width modulation(PWM) voltage-source converter (VSC) which controls the dc-link voltage and exchanges the reactive to the MG;
- DC–DC buck/boost converter which controls the real power;
- Electric double layer capacitor (EDLC) Based on the requirement of the dc–dc Buck/boost converter which can charges or discharges the amount of energy.

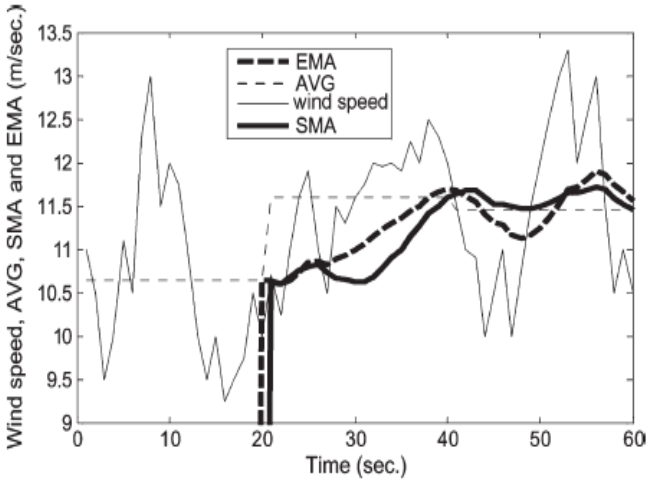

Fig 4. Comparison among AVG, SMA, and EMA.

Modeling and Control Strategies of PWM VSC: Here R and X, are the coupling transformer resistance and reactance. The phasor quantities and V_C and I represent the output ac voltage of the VSC and the current flowing from the MG to the VSC, respectively. V_K represents the MG's voltage at point k where the ultra-capacitor is connected as shown in Fig. 9. The mathematical description and equations of the active power P and the reactive power Q which flow through the VSC can be found in our previous work [15].

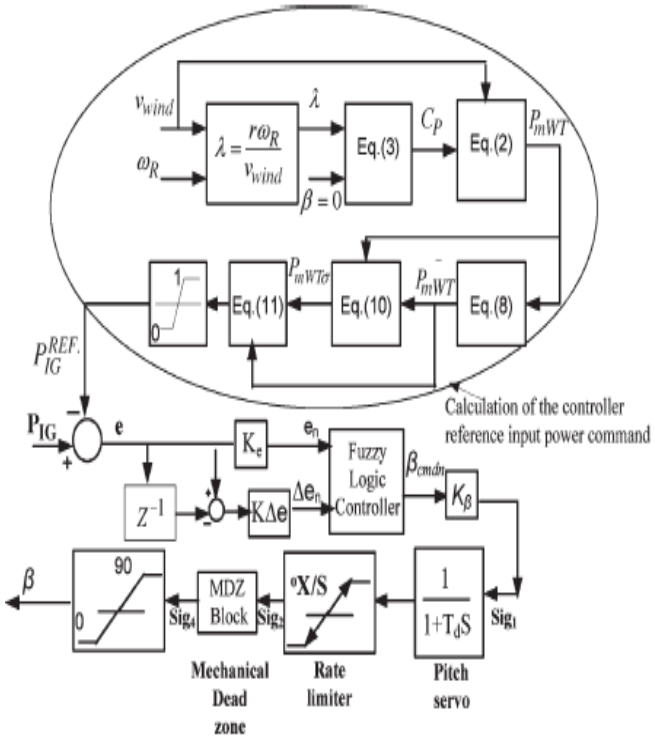

Fig. 5. Fuzzy logic pitch controller for smoothing wind power.

Modeling of a DC–DC Buck/Boost Converter: The dc–dc buck/boost converter shown in Fig. 10 can operated alternately by controlling switches g1 and g2 to be ON or OFF. In the boost converter mode generated wind power PIG is less than the reference power, EDLC is discharged and the ECS injects power to the wind generator bus. In buck converter mode generated wind power is PIG exceeds the reference value, EDLC is charged and ECS absorbs the power generated by the wind generator and the MG.

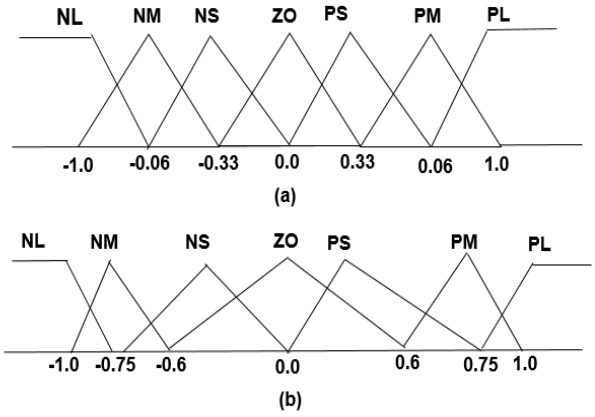

Fig. 6. Fuzzy sets and their corresponding membership functions. (a) Inputs($e_n$and Δe_n). (b) Output (β_{cmd}).

TABLE I: Fuzzy Rules Of The Pitch Controller

β_{cmd}	Δe_n NL	NM	NS	ZO	PS	PM	PL
NL	NL	NL	NM	NM	NS	NS	ZO
NM	NL	NM	NM	NS	NS	ZO	PS
e_n NS	NM	NM	NS	NS	ZO	PS	PS
ZO	NM	NS	NS	ZO	PS	PS	PM
PS	NS	NS	ZO	PS	PS	PM	PM
PM	NS	ZO	PS	PS	PM	PM	PL
PL	ZO	PS	PS	PM	PM	PL	PL

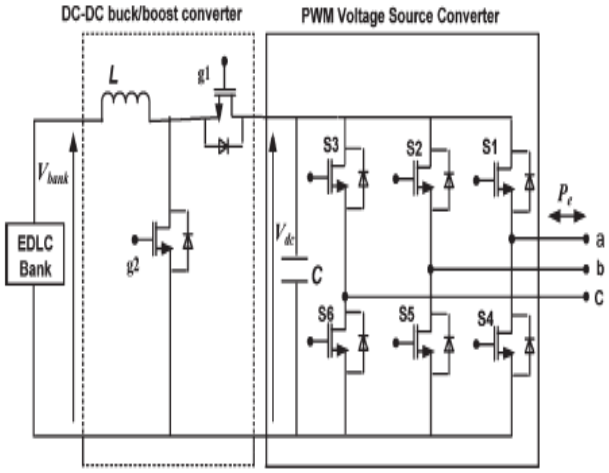

Fig. 7. Schematic diagram of an ECS.

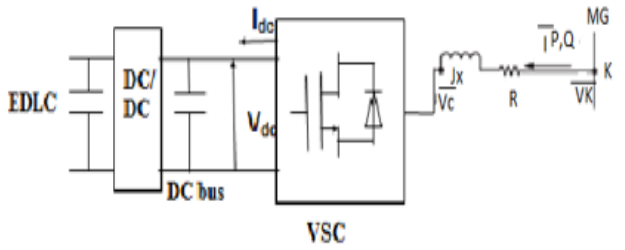

Fig. 8. Equivalent circuit of a VSC including a coupling transformer.

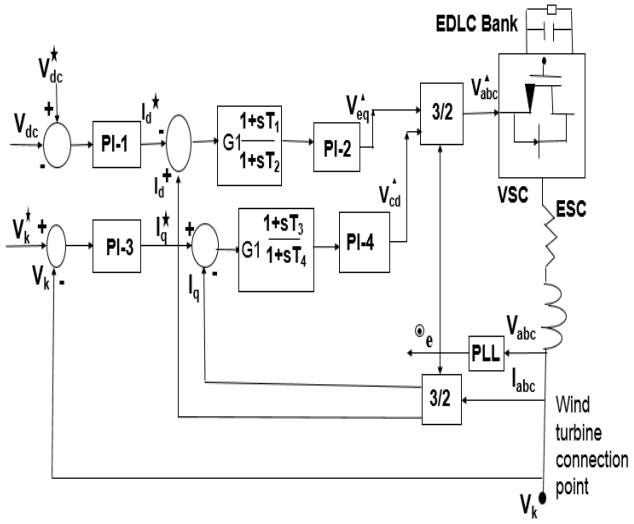

Fig. 9. VSC block diagram control.

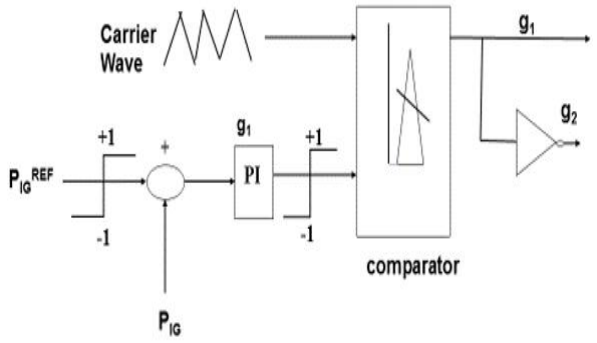

Fig. 10. Control block of a dc–dc buck/boost converter.

D.DFIG

The DFIG is constructed from a wound rotor asynchronous machine shown in fig.11. Variable speed operation is obtained by injecting a variable voltage into the rotor at slip frequency. The injected rotor voltage is obtained using two AC/DC insulated gate bipolar transistors (IGBT) based voltage source converters (VSC), linked by a DC bus. The converter ratings determine the variable speed range. The gearbox ratio is set so that the nominal speed of the IG corresponds to the middle value of the rotor-speed range of the wind turbine. This is done in order to minimize the size of the inverter in the rotor circuit which will vary with the rotor speed range. With this inverter it is possible to control the speed (or the torque) and also the reactive power on the stator side of the induction generator (IG). The speed range, i.e., the slip, is approximately determined by the ratio between the stator to rotor voltage. The stator to rotor turns ratio can be designed so that maximum voltage of the inverter corresponds to the desired maximum rotor voltage to get the desired slip.

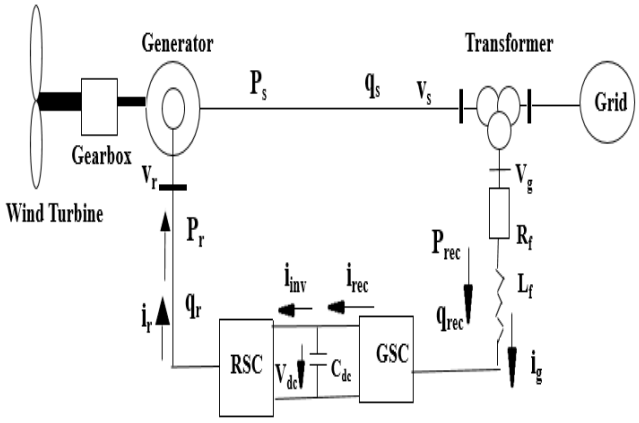

Fig.11.The DFIG wind turbine system.

E. Nickel-cadmium Batteries

The abbreviation of Ni-Cd is derived from the chemical symbols of nickel (Ni) and cadmium (Cd) as shown in Fig.12. Nickel cadmium battery is a type of recharging battery,have excellent performance characteristics at low temperatures. Nickel-cadmium batteries contains high charge and discharge rates.

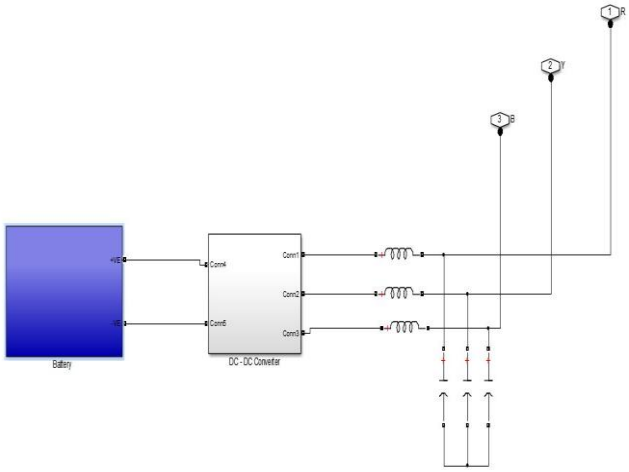

Fig.12. Nickel-cadmium batteries block diagram.

F. Solid Oxide Fuel Cell

Solid oxide fuel cells (SOFCs) offer a clean, low-pollution technology to the electrochemically generated power at high efficiencies these are providing many advantages over traditional energy conversion systems including high efficiency, reliability, modularity, fuel adaptability, and verylow levels of NOx and SOx emissions as shown in Fig.13. Vibration -free operation of SOFCs also eliminates noise usually associated with conventional power generation systems having temperature range of 900 to 1000^0c.

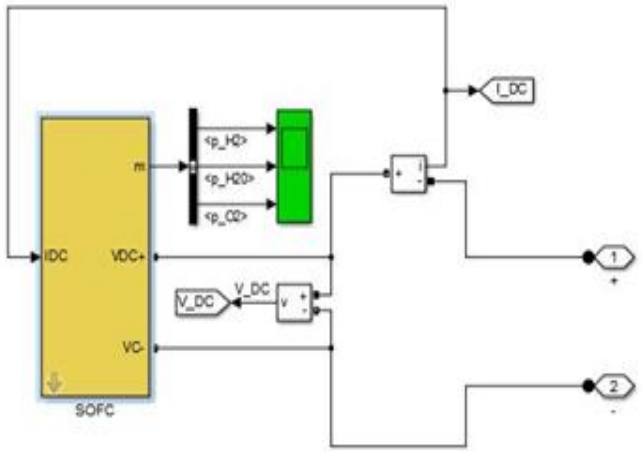

Fig.13. SOFC block diagram.

V. RESULTS

To maintain the stability of a micro grid by reducing frequency fluctuations by using fuzzy logic pitch angle controller can smooth the fluctuations of generated power even at wind speed and generated power less than nominal value and follow the reference signal produced by EMA. ECS completely compensated any fluctuation in the generated wind power and kept the reactive power absorbed from the MG can maintain reactive power to zero. We are placing nickel cadmium battery in place of lead-acid batteries because these are having high charging and discharging powers and long life. When the nickel-cadmium batteries are installed in the MG, the frequency deviation was small because batteries injected the most percentage of the power lost due to islanding. The fuzzy logic pitch controller, ECS technique, and nickel-cadmium batteries solid oxide fuel cell were not activated during the interconnected mode (i.e., before t = 70 s). This is because, in the interconnected mode, any fluctuations on the wind generation output power can be easily supported by the main grid. SOFC and nickel-cadmium batteries contains high discharging power and these are having long life and results as shown in Figs.14 and 15.

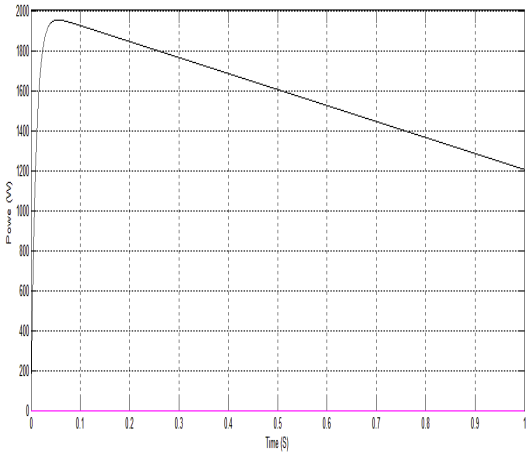

Fig.14. Active power and reactive power by using SOFC, Ni-Cd batteries.

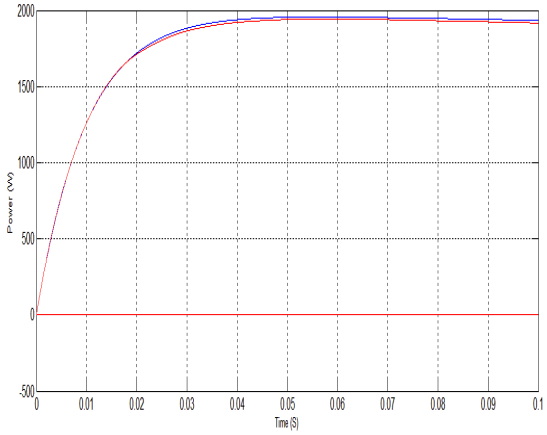

Fig.15. comparison between proposed method and existing method.

VI. CONCLUSION

In this paper, the fuzzy logic pitch angle controller can smooth the wind power fluctuations partially. The ECS controller was used to completely remove the fluctuations of the frequency, voltage, and active and reactive power resulting from the wind power fluctuations inside the MG. However, the results showed that the performance of the ECS controller is better than that of the fuzzy controller; the cost of the fuzzy controller is much lower than that of the ECS controller. When nickel-cadmium batteries were inserted in the MG, the rated energy and the rated power of the required fly wheel are dramatically reduced. That is because most of the power required in the MG subsequent islanding occurrence will be provided by the Nickel-cadmium batteries. Therefore, the MG can stay in the islanding mode for a time longer than that in the cases without nickel-cadmium batteries. SOFC is a high efficient and reliable fuel cell working at high and low temperatures, Based on the obtained results, we conclude that a specific strategy is more suitable than the others for specific applications.

VII. REFERENCES

[1] R. M. Kamel, A. Chaouachi, and K. Nagasaka, "Carbon emissions reduction and power losses saving besides voltage profiles improvement using micro grids," Low Carbon Economy J., vol. 1, no. 1, pp. 1–7, Sep. 2010.

[2] R. M. Kamel, A. Chaouachi, and K. Nagasaka, "Design and testing of three earthing systems for micro-grid protection during the islandingMode," Smart Grid Renewable Energ. J., vol. 1, no. 3, pp. 132–142, Dec. 2010.

[3] C. L. Moreira, F. O. Resende, and J. A. P. Lopes, "Using low voltage micro grids for service restoration," IEEE Trans. Power Syst., vol. 22,no. 1, pp. 395–403, Feb. 2007.

[4] H. A. Gil and G. Joos, "Models for quantifying the economic benefits of distributed generation," IEEE Trans. Power Syst., vol. 23, no. 2, pp. 327– 335, May 2008.

[5] Y. M. Atwa and E. F. El-Saadany, "Reliability evaluation for distribution system with renewable distributed generation

during islanded modeof operation," IEEE Trans. Power Syst., vol. 24, no. 2, pp. 572–581, May 2009.
[6] A. Piccolo and P. Siano, "Evaluating the impact of network investment\ deferral on distributed generation expansion," IEEE Trans. Power Syst., vol. 24, no. 3, pp. 1559–1567, Aug. 2009.
[7] E. Denny and M. O'Malley, "Wind generation, power system operation, emissions reduction," IEEE Trans. Power Syst., vol. 21, no. 1, pp. 341– 347, Feb. 2006.
[8] J. Lopes, C. L. Moreira, and A. G.Madureira, "Defining control strategies for micro grids islanded operation," IEEE Trans. Power Syst., vol. 21, no. 2, pp. 916–924, May 2006.
[9] F. Kanellos, A. I. Tsouchnikas, and N. D. Hatziargyriou, "Micro-grid simulation during grid-connected and islanded modes of operation," presented at the Int. Conf. Power Systems Transients (IPST), Montreal, QC, Canada, Jun. 19–23, 2005, Paper IPST05-113.
[10] S. Barsali, M. Ceraolo, P. Pelacchi, and D. Poli, "Control techniques of dispersed generators to improve the continuity of electricity supply," in Proc. PES Winter Meeting, 2002, vol. 2, pp. 789–794.
[11] F. Katiraei, M. R. Iravani, and P. W. Lehn, "Micro-grid autonomous operation during and subsequent to islanding process," IEEE Trans. PowerDel., vol. 20, no. 1, pp. 248–257, Jan. 2005.
[12] D. Georgakis, S. Papathanassiou, N. Hatziargyriou, A. Engler, and C. Hardt, "Operation of a prototype microgrid system based on microsources equipped with fast-acting power electronics interfaces," in Proc.IEEE 35th PESC, Aachen, Germany, 2004, vol. 4, pp. 2521–2526.
[13] T. Tran-Quoc, N. Hadjsaid, G. Rami, L. Le-Thanh, L. Bernard, G. Verneau, J. L. Mertz, C. Corenwinder, P. Michalak, and M. Boll,"Dynamic analysis of an insulated distribution network," in Proc. IEEE Power Syst. Conf. Expo., Oct. 10–13, 2004, vol. 2, pp. 815–821.
[14] R. Caldon and R. Turri, "Analysis of dynamic performance of dispersed generation connected through inverters to distribution networks," in Proc.17th Int. Conf. Elect. Distrib., Barcelona, Spain, May 12–15, 2003.
[15] R. M. Kamel, A. Chaouachi, and K. Nagasaka, "Wind power smoothing using fuzzy logic pitch controller and energy capacitor system for improvement micro-grid performance in islanding mode," Energy, vol. 35, no. 5, pp. 2119–2129, May 2010.
[16] R. M. Kamel, A. Chaouachi, and K. Nagasaka, "Three proposed control techniques applied upon inverters which interfacing micro sources with the islanded micro grid (MG)," ISESCO Sci. Technol. Vis., vol. 7, no. 11, pp. 76–84, May 2011. 1322 IEEE TRANSACTIONS ON INDUSTRIAL ELECTRONICS, VOL. 60, NO. 4, APRIL 2013
[17] R. M. Kamel, A. Chaouachi, and K. Nagasaka, "Detailed analysis of micro-grid stability during islanding mode under different load conditions," Eng. J., vol. 3, pp. 508–516, May 2011.
[18] Y. Zhu and K. Tomsovic, "Development of models for analyzing the loadfollowing performance of microturbines and fuel cells," Elect. Power Syst.Res., vol. 62, no. 1, pp. 1–11, May 2002.
[19] J. Padullés, G. W. Ault, and J. R. McDonald, "An integrated SOFC plantdynamic model for power systems simulation," J. Power Sources, vol. 86,no. 1/2, pp. 495–500, Mar. 2000.
[20] N. Hatziagyriou, F. Kanellos, G. Kariniotakis, X. Le Pivert, N. Jenkins, N. Jayawarna, J. Pecas Lopes, N. Gil, C. Moreira, J. Oyarzabal, andJ. Z. Larrabe, "Modeling of micro-sources for security studies," in Proc.CIGRE Session, Paris, France, 2004.
[21] N.Prema kumar, K. Nirmala Kumari,K.M. Rosalina "Modeling Design of Solide Oxide Fuel Cell Power System for Distributed Generation Applications" IJARCET-2012.

Author's Profile:

P.Tejaswi received B.Tech(E.E.E) from Sri Sai Institute of Technology and Science at Rayachoty in 2013, Presently pursuing M.Tech(EPS) at Madanapalle Institute of Technology and Science, Madanapalle, her areas of intrest towards Renewable power Generation and Distribution.